Neuron 51, 661–670, September 7, 2006 ©2006 Elsevier Inc. DOI 10.1016/j.neuron.2006.07.021

The Radial Bias: A Different Slant on Visual Orientation Sensitivity in Human and Nonhuman Primates

Yuka Sasaki,[1,2,3,*] Reza Rajimehr,[1] Byoung Woo Kim,[1] Leeland B. Ekstrom,[1,4] Wim Vanduffel,[1,2] and Roger B.H. Tootell[1,2,4]

[1] Athinoula A. Martinos Center for Biomedical Imaging
Department of Radiology
Massachusetts General Hospital
149 13th Street
Charlestown, Massachusetts 02129

[2] Department of Radiology
Harvard Medical School
25 Shattuck Street
Boston, Massachusetts 02115

[3] ERATO Shimojo Implicit Brain Function Project
California Institute of Technology
Pasadena, California 91125

[4] Health Sciences and Technology/
Nuclear Science and Engineering
Massachusetts Institute of Technology
77 Massachusetts Avenue
Cambridge, Massachusetts 02139

Summary

It is generally assumed that sensitivity to different stimulus orientations is mapped in a globally equivalent fashion across primate visual cortex, at a spatial scale larger than that of orientation columns. However, some evidence predicts instead that radial orientations should produce higher activity than other orientations, throughout visual cortex. Here, this radial orientation bias was robustly confirmed using (1) human psychophysics, plus fMRI in (2) humans and (3) behaving monkeys. In visual cortex, fMRI activity was at least 20% higher in the retinotopic representations of polar angle which corresponded to the radial stimulus orientations (relative to tangential). In a global demonstration of this, we activated complementary *retinotopic* quadrants of visual cortex by simply changing stimulus *orientation*, without changing stimulus location in the visual field. This evidence reveals a neural link between orientation sensitivity and the cortical retinotopy, which have previously been considered independent.

Introduction

Since stimulus orientation selectivity was first discovered in visual cortex (Hubel and Wiesel, 1962), it has become universally accepted that all orientations are represented in the cortical map, in each part of the visual field. Most models assume further that all orientations are represented in an *equally balanced*, equivalent representation, throughout the cortical map; this is certainly the simplest computational model. Indeed, a *lack* of global orientation bias has often been used as the null hypothesis (Haynes and Rees, 2005; Kamitani and Tong, 2005; Schoups et al., 2001).

*Correspondence: yuka@nmr.mgh.harvard.edu

However, there have also been competing reports suggesting a global variation in orientation sensitivity. Earlier studies concentrated on a small bias for vertical and horizontal orientations, the so-called "oblique effect" (Furmanski and Engel, 2000; Mansfield, 1974; Orban et al., 1984).

Here, we describe imaging evidence for a different (but compatible) effect: a bias for radial orientations (i.e., those that are collinear with a line intersecting the center of gaze). Previous evidence for a radial orientation bias has been reported from anatomical and physiological studies in retina, LGN, and cortex in cat (Leventhal and Schall, 1983; Levick and Thibos, 1982) and monkey (Schall et al., 1986), and in human psychophysics (Bennett and Banks, 1991; Berardi and Fiorentini, 1991; Fahle, 1986; McGraw and Whitaker, 1999; Rovamo et al., 1982; Scobey and van Kan, 1991; Temme et al., 1985; Westheimer, 2003, 2005; Yap et al., 1987). Nevertheless, this previous evidence for a radial bias has been largely ignored in current expectations about orientation tuning in primate cortex.

The present study demonstrates that a strong radial orientation bias is present in fMRI from both human and monkey subjects and in related psychophysical studies. Unlike the oblique effect, the radial bias in orientation sensitivity demonstrates a specific relationship between the retinotopy and the orientation tuning throughout visual cortex, which has not been described previously.

Results

Psychophysics

First we describe evidence for an enhanced sensitivity to radial orientations in human perception, based on psychophysics. We tested this in four subjects, using stimuli adapted from corresponding fMRI studies (see below). Contrast sensitivity (the inverse of contrast detection threshold) was measured for small, peripherally located grating patches. Sensitivity to radial versus tangential orientations was measured in eight equally peripheral locations, each separated by 45° of polar angle (Figure 1A), using a temporal two-alternative forced choice paradigm (see Experimental Procedures). Sensitivity was significantly higher to radial orientations than to tangential orientations ($p < 0.0001$; ANOVA; see Figure 1B); this and previous psychophysics (ibid.) strongly supports the radial orientation hypothesis. In addition, Figure 1B supports previous evidence for the well-known oblique effect, which is different from (though conceptually compatible with) the radial orientation effect tested here.

Human fMRI

The radial orientation bias (e.g., Figure 1) predicts a large-scale variation in orientation sensitivity across fMRI maps in visual cortex, unlike any described previously. Specifically, increased neural activity to radial *orientations* should produce higher brain activity along the corresponding polar angles in the *retinotopic* map.

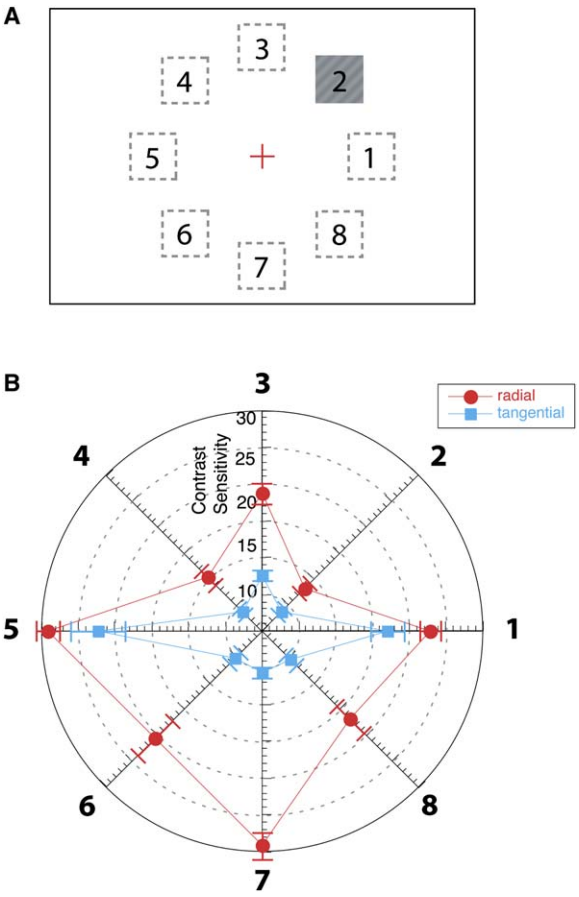

Figure 1. Psychophysical Testing Shows a Higher Contrast Sensitivity for Radial Orientations, Compared to Tangential Orientations

(A) Stimulus configuration. A small grating patch was presented peripherally. In the example here, the grating orientation was radial, and it was located in the upper right visual field, in position #2. In the actual experiments, a patch of either radial or tangential orientation was presented at each of eight possible locations, indicated by dotted lines, relative to the fixation point (central cross).

(B) Results. Contrast sensitivity (the inverse of contrast detection threshold) is plotted, at each of eight locations. Error bars represent one standard error of the mean. When we applied a repeated measure of ANOVA with orientation (radial and tangential) and location (eight possible locations) as factors, the test revealed a significant main effect of orientation ($df = (1, 7)$, $p < 0.0001$). The interaction of orientation and location ($df = (7, 24)$, $p < 0.025$) demonstrated that the sensitivity for radial orientations was significantly better than that for tangential orientations. Because the interaction indicated that the sensitivity depends on visual field position, we further analyzed that effect. The apparent sensitivity difference between the upper and lower visual fields did not reach statistical significance. Sensitivity along horizontal and vertical meridians was significantly better than that for oblique meridians ($p < 0.05$), consistent with the well-known oblique effect.

However, according to conventional assumptions, gratings of different orientation should instead produce *no* systematic large-scale differences in brain activity: this was the null hypothesis.

To test this, six fMRI subjects were presented with contrast-reversing, phase-shifting gratings presented at two orthogonal orientations (one orientation at a time), while maintaining fixation on the center of the gratings. The gratings were matched on all other stimulus features (stripe width, contrast, temporal variation, and grating size/position). Importantly, there was no retinotopic variation in these stimuli; the size and position of the display remained constant throughout the experiment.

We first describe the effects of orthogonal oblique orientations. The radial orientations of these gratings occur only in alternating quadrants of the stimuli, and the quadrants including radial stripes are spatially complementary (i.e., they are perpendicular to each other). By our radial orientation hypothesis, cortical activity should be relatively higher in the retinotopic regions which represent these radial stripes. To test this prediction, we took advantage of a specific feature of the retinotopic maps. In primate visual cortex, there exist corresponding, alternating maps of the visual field quadrants (see Figures 2A and 2B). Therefore, by simply changing the stimulus *orientation* (but *not* stimulus location), any radial orientation bias should preferentially activate these alternating *retinotopic* quadrants of the visual cortical map (see Figures 2C and 2D).

Figure 3B confirms this remarkable result in one representative human subject. Comparison of Figures 2 and 3B verifies that this "checkerboard" activity pattern is located in the predicted retinotopic quadrants of visual cortex, as measured in independent tests of the retinotopy from the same subject(s). These fMRI differences were quite robust (19.8%, comparing radial versus tangential orientations) even when averaged across subjects (see Figure 4A)—despite the imperfect alignment of such data across retinotopic boundaries. The similarities between the psychophysics and fMRI are quite striking (c.f. Figures 4B and 4C), if one allows for differences in the scales compared.

Monkey fMRI

Most of our understanding about the neural basis of orientation tuning is based on electrophysiological studies in cats or monkeys, not from human fMRI. Perhaps this fMRI-based radial orientation bias is a specialization of human cortex, which is lacking in "lower" mammals? To test this, we repeated the above fMRI experiments in two awake behaving macaque monkeys, using the same scanner, analysis tools, and general procedures as in the human experiments. Results were very similar in the two families of primates (e.g., Figures 3B, 3C, and 5). Despite 25 million years of evolutionary separation between humans and macaques, the monkeys showed essentially the same orientation-retinotopy relationship as the humans. This suggests that the radial orientation bias is a fundamental, evolutionarily conserved component of primate visual cortex.

Detailed Relationship between Orientation and Retinotopy

The scheme in Figure 2 predicts an even more elegant relationship between the orientation and retinotopic maps, when viewed at higher magnification. Recall that each of the large regions in Figure 2B is actually comprised of approximately four adjacent but similar maps of a common visual field quadrant. Thus, a radial orientation bias should also show up as activated cortical stripes corresponding to the specific retinotopic polar angle *within* each area (e.g., the stripes in Figure 2D)—as well as in the larger blocs of cortex colored in Figure 2B.

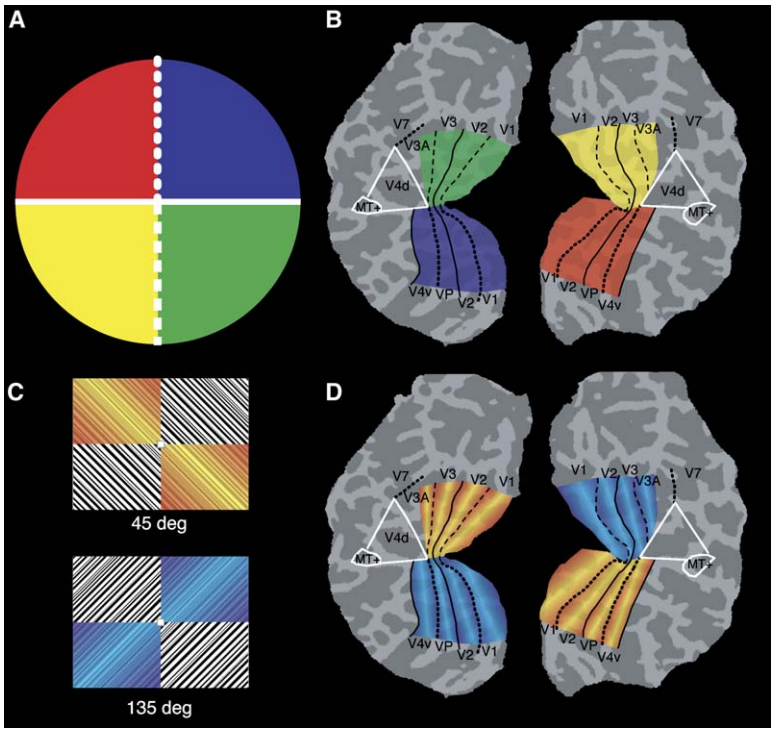

Figure 2. The Radial Orientation Hypothesis Predicts that Gratings of Orthogonal Oblique Orientation Will Selectively Activate the Retinotopic Representations of Orthogonal Visual Field Quadrants

To illustrate this prediction, (A) divides the visual field into quadrants, indicated by arbitrarily assigned colors. Solid lines indicate the retinotopic representation of the horizontal meridian, dotted lines indicate the upper vertical meridian, and dashed lines indicate the lower vertical meridian.

(B) A map of corresponding visual field representations in human visual cortex (flattened right and left hemisphere on the right and left respectively), acquired from a representative subject using conventional fMRI retinotopic mapping. Thus, when one stares at the center of (A), stimuli in the upper left of the visual field (red) produce activity in the lower right of the flattened cortex ([B], red), and similarly for each of the other colors.

At a finer level of analysis, each of the color-coded cortical "quadrants" is comprised of four repeated maps of that same visual field quadrant. For example, the upper left (red) visual field is represented in each of four cortical areas (V1v, V2v, V3v, and V4v). However, since these four cortical areas lie adjacent to each other, the overall retinotopic organization shown in (B) remains true. The retinotopic mapping is similar in macaque monkey (e.g., Figure 5).

(C) Examples of the stimuli used in the orientation tests. Pseudocolor has been added here to illustrate that only alternating visual field quadrants contain radial orientations; the actual experimental stimuli were black-white.

(D) The activation predicted by the gratings in (C), with the location of the retinotopic visual areas included. Consistent with the radial orientation hypothesis and the retinotopic map, the relative activity differences produced by the orthogonal orientations should reverse in sign between hemispheres, and the radial orientation bias should extend over most or all of the retinotopic cortical areas.

This higher-magnification result was tested first by measuring the fMRI activity produced by horizontal gratings, compared to that produced by vertical gratings. Consistent with the model's predictions (see Figures 6A and 6B), we found that vertical stimulus orientations produced highest activity along the retinotopic representation of the vertical meridian, whereas horizontal orientations produced highest activity along the horizontal meridian representation (Figures 6C–6F). These results again support the radial orientation hypothesis: those few stripes which pass through (or at least near) the center of gaze produced the greatest fMRI activity, in their corresponding retinotopic representations in cortex. This enhancement to radial orientations occurred in most or all of the retinotopic visual areas, especially the most retinotopically specific areas with small receptive fields (V1, V2, V3). A similar bias was seen in the comparisons between the oblique orientations: the highest activity produced by each oblique grating was again found in bands, corresponding to the appropriate retinotopic polar angle representation, wedged *between* the bands produced by vertical and horizontal orientations (e.g., Figure 7). Again, this represents higher activity to the subset of radial stripes within the overall stimulus grating.

Additional Controls, Attention

Could visual attention instead account for this orientation-specific bias? Is attention somehow "drawn" along the radial stripes, in our passive viewing conditions? To test this, we cued human subjects to report the presence or absence of a small probe target, embedded within the grating stimuli, in fMRI tests otherwise similar to those above. When present (50% of trials), the probe target was a small, red dot which could appear anywhere within the grating, with equal spatial weighting. Within a single presentation, the probe dot was located in white not black stripes (so that detection remained stable), but over time, every pixel on the screen could be included within a white or black stripe, with 50% probability. The dot detection task was made quite challenging by varying the red-white ratio (roughly, saturation) of the dot, using a staircase threshold converging on 68% correct. This task diverted attention from the grating orientation per se (since grating orientation was irrelevant for successful dot detection), while concurrently directing attention equally across the whole stimulus grating. This control for attention did not significantly change our results (Figures 8A and 8B). At least in this test, the radial orientation bias apparently reflects sensory filtering properties, relatively uncontaminated by uncontrolled attention.

Additional Controls, Event-Related

In neurophysiological studies of orientation tuning, stimuli are normally presented for a relatively short time (e.g., 200–2000 ms). Here, we also presented each individual grating for a relatively short time (500 ms), but multiple gratings of the same orientation were presented within longer blocks (16 s). Is it possible that orientation

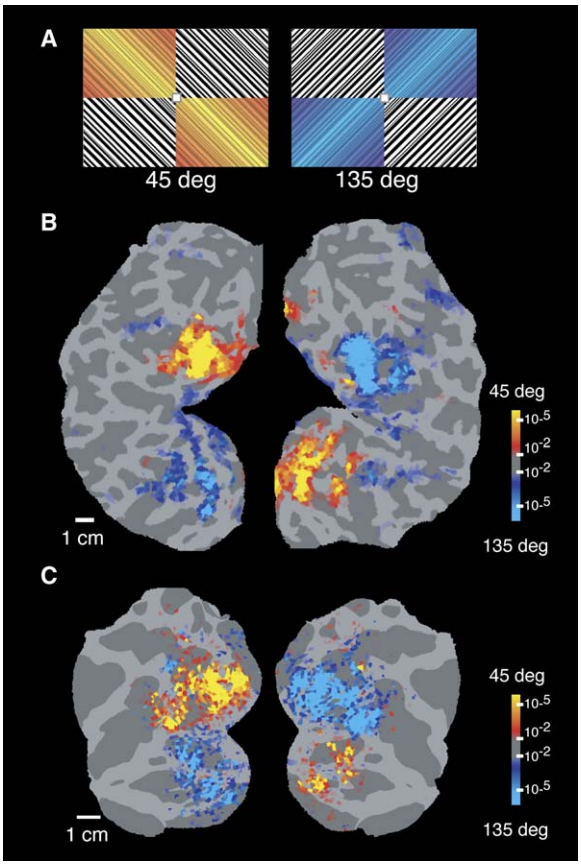

Figure 3. As Predicted, Gratings of Orthogonal Oblique Orientation Activate Complementary Quadrants in Visual Cortex, in Human and Nonhuman Primates

(A) Examples of the stimuli used in this experiment. Subjects fixated the center of both stimuli, which extended over the entire visual field representation activated in (B) and (C). As in Figure 2, color has been added here to the experimental stimuli, to clarify the relationship between the stimuli and the corresponding cortical activation (B and C).

(B) The activity maps from the left and right hemispheres of the human subject whose right hemisphere is illustrated in Figure 2 (to facilitate comparison to the experimental prediction). As in the icon (top, [A]), significantly higher activity in response to the 10:30–4:30 oblique orientation (45°) is shown in red-yellow pseudocolor; higher activity to the orthogonal oblique grating is blue-cyan. As predicted, fMRI activity produced by this change in orientation is relatively higher in complementary cortical quadrants. The color bar to the right indicates the statistical significance of the fMRI activation.

(C) The analogous fMRI result, produced by the same stimuli, from the analogous regions of cortex, in an awake fixating monkey. Figure conventions (and most experimental details) are as in (B).

sensitivity varies in a time-specific manner, such that the biases shown here manifest themselves only after several seconds? (On a much shorter time scale, orientation sensitivity has been shown to vary dynamically [Ringach et al., 1997]). To test this, we remeasured the bias using event-related fMRI techniques, with grating presentations limited to 0.5–1 s. Again, we found the same radial orientation bias (Figure 8C).

Additional Controls, Averaging across Subjects

These within-area radial orientation biases were also robust when data were averaged across all subjects, for those retinotopic areas which were adequately aligned (e.g., V1–V2 and V2–V3 boundaries; Figure 8D).

Global (Nonretinotopic) Tests

To confirm the radial effect even further, it would be ideal to measure fMRI activation in response to radial gratings, compared to that produced by conventional rectilinear gratings. Unfortunately, the geometry of the two grating types makes direct comparisons problematic: the component stripe width varies with eccentricity in the radial gratings, but not in the conventional gratings (see Figure S1 in the Supplemental Data available with this article online). Differences in stimulus stripe width are known to affect cortical activity via differences in spatial frequency sensitivity (Albrecht et al., 1980; Movshon et al., 1978; Tootell et al., 1988), which also varies with eccentricity (De Valois et al., 1982a; Frisen and Glansholm, 1975; Sasaki et al., 2001). Thus a direct comparison between radial and rectilinear gratings could reflect such differences in spatial frequency sensitivity, rather than a radial preference per se.

To circumvent such confounds, we compared fMRI activity produced by the conventional and rectilinear gratings using transitivity (i.e., if A < B and B < C, then A < C). The common standard (B) was a concentric grating, otherwise equated to the grating of interest (using either scaled stripe width in the comparison with the radial grating or constant stripe width in the comparison with the rectilinear grating). We found that concentric gratings produced significantly more activity than matched rectilinear gratings, and radial gratings produced marginally more activity than matched concentric gratings ($p < 0.01$; see Figure S1). This confirmed our earlier conclusion, that primate visual cortex is especially responsive to radial orientations. Additional experiments confirmed that enhanced responses to concentric gratings occurred only when the gratings were centrally fixated—i.e., when the "polar" gratings were actually polar, relative to the cortical map.

Retinotopically Limited Stimuli

In neurophysiological studies of orientation tuning, stimuli are often confined to a retinotopically restricted receptive field. In one subject, we tested whether the radial bias remains using similar stimuli. The results were generally consistent with all the other experiments in this study (Figure S2). The radial bias apparently remains in the fMRI, even when stimuli are retinotopically restricted within four small patches, as in our psychophysical experiments (e.g., Figures 1 and 3). In this preliminary test, the orientation bias was less robust than that using large-field stimuli; this may reflect the unavoidable confounding of spatial location and (orientation nonselective) stimulus borders in the fMRI measurements.

Discussion

The radial effect described here was quite robust. When averaged across subjects, fMRI amplitudes were ~20% higher when produced by oblique orientations that were radial, compared with tangential (Figure 4). Since those "radial" measurements also included orientations up to 45° from radial, the corrected fMRI difference for strictly radial orientations may be significantly larger (if linear,

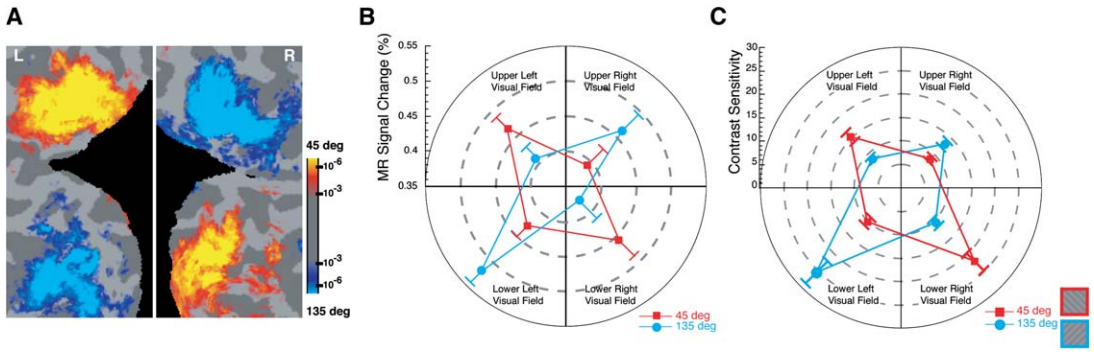

Figure 4. Responses to Orthogonal Oblique Orientations, Averaged across Subjects, in fMRI and Psychophysics

(A) fMRI activity in flattened left and right hemispheres of visual cortex (as in Figures 2D and 3B), in response to two orthogonal oblique orientations (e.g., Figures 2C and 3A), averaged across all subjects tested (map threshold, $p < 0.001$). The same biases shown in the individual subject (Figure 3B) are confirmed in this average across subjects.

(B) Amplitude of MR signal changes averaged from cortical areas V1, V2, and V3, corresponding to each visual field quadrant, averaged across subjects.

(C) Psychophysical data from corresponding regions of the visual field (as in Figure 1), also averaged across subjects. Note the similarity between (B) and (C), despite the difference in scale across the two dimensions.

Error bars represent one standard error of the mean.

~40%). The radial bias was found in all subjects tested (n = 6 in human fMRI, plus an additional n = 4 from human psychophysics, plus n = 2 in macaque fMRI).

The psychophysical oblique effect bears a superficial resemblance to the present radial orientation effect, but that resemblance is misleading: the two effects are actually quite different. First, in the oblique effect, there is a higher sensitivity to both vertical and horizontal ("cardinal") orientations, compared to that for oblique orientations. In contrast, the radial bias assumes no superiority for cardinal orientations. This is borne out by the present imaging evidence, which shows strong differences for all orthogonal polar angles, not just the vertical and horizontal ones. Second, the orientation bias in the oblique effect is assumed to extend over the entire visual field (but see Berkley et al. [1975])—not just along

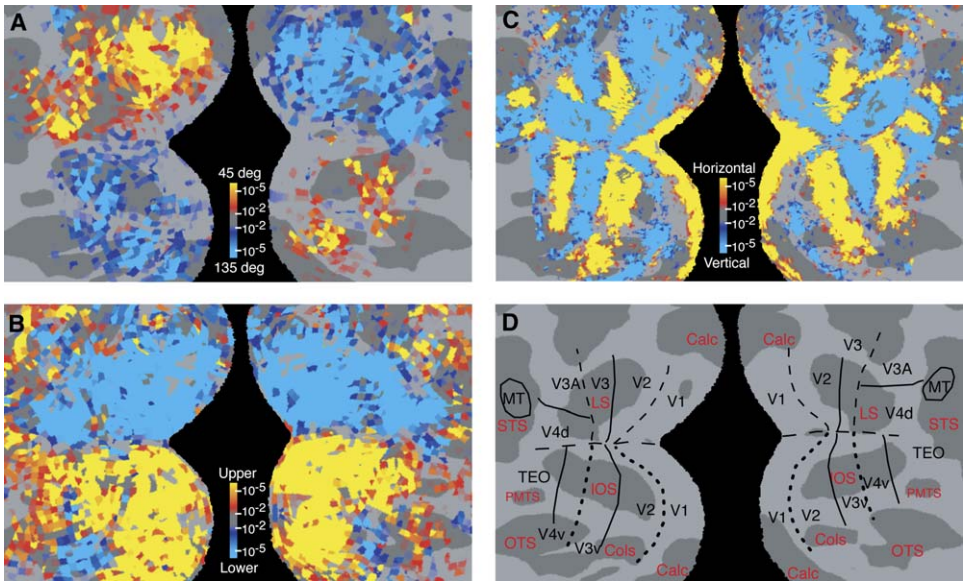

Figure 5. Retinotopic Confirmation of the Radial Orientation Effect in Macaque Monkey

(A) Magnified view of Figure 3C, showing activity differences in response to orthogonal oblique orientations. As in the human experiments, the monkey fixated the center of the gratings, near continuously throughout the fMRI acquisitions (e.g., Figure 1 of Vanduffel et al. [2001]). To confirm that these variations in fMRI activity matched the specific predictions of the radial orientation hypothesis, we also activated the representation of the upper and lower visual fields (B) and the vertical and horizontal meridians (C), using fMRI coupled with retinotopically varying stimuli (Fize et al., 2003) in the same fixating monkey, in separate experiments. This revealed the location of the retinotopy and cortical areas in the same cortical tissue ([D] solid lines indicate the retinotopic representation of the horizontal meridian, dotted lines indicate the upper vertical meridian, and dashed lines indicate the lower vertical meridian). As predicted, the relative activity differences produced by the orthogonal orientations reversed in sign between hemispheres and along the retinotopic division between upper and lower visual fields. The radial orientation bias included essentially all the retinotopic visual areas. On-line recordings of eye movements and the abrupt functional transition in the foveal representation of the retinotopic maps (e.g., [B] and [C]), confirmed that central visual fixation remained near-constant during the fMRI acquisitions.

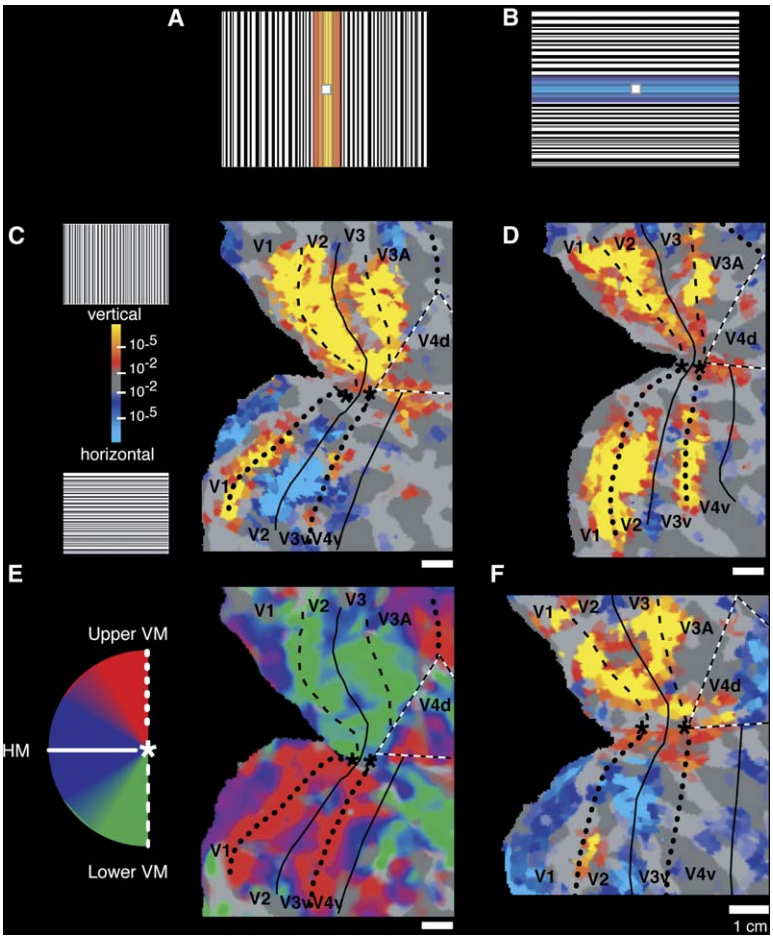

Figure 6. fMRI Reveals a Systematic Relationship between Orientation Sensitivity and the Retinotopic Map in Visual Cortex, Based on Enhanced Activity to Radial Orientations

The top panels are examples of the grating stimuli used here, oriented either vertically (A) or horizontally (B). Again, color was not present in the actual experimental stimuli, but pseudocolor has been superimposed on the stimuli here, to indicate the location of radial stripes. In response to the vertical grating, any enhanced responsiveness to radial orientations will produce higher activity along the vertical retinotopic meridian. In the horizontal grating, the radial stimulus stripes (and the predicted enhancement of activity) are rotated 90°.

(C–F) Topography of fMRI activity in human visual cortex from the right hemisphere, in flattened cortical maps.

(C, D, and F) From three different subjects; each shows significant increases in activity produced by gratings of either vertical orientation (red-yellow) or horizontal orientation (blue-cyan) in different cortical regions.

(E) Representative map of phase-encoded polar angle retinotopy, from the hemisphere also shown in (C). As in other figures, solid lines indicate the retinotopic representation of the horizontal meridian in the same subject, dotted lines indicate the upper vertical meridian, and dashed lines indicate the lower vertical meridian (logo, leftmost panel [E]).

As predicted by the radial orientation hypothesis (A and B), the vertical grating produced relatively higher activity along retinotopic representations of the vertical meridian (e.g., borders of V1–V2, V3–V4v, V3–V3A). The horizontal grating produced higher activity along representations of the horizontal meridian (e.g., V2–V3 border, midline of V1).

the radial axes, as shown here. Third, physiological evidence for the oblique effect has been reported only in V1 (De Valois et al., 1982b; Furmanski and Engel, 2000), whereas the radial effect demonstrated here was found in essentially all retinotopic areas. Thus, the oblique effect is different from (though logically compatible with) the radial orientation effect described here.

Given the robust nature of this effect, why is the radial orientation bias not already well described in the current literature? One possibility is that the fMRI is revealing neural feature(s) which are subtle or missing in classic neurobiological measurements. fMRI reflects changes in hemodynamics, whereas single units measure extracellular action potentials, and the correlation between these two measurements is imperfect (e.g., Kim et al. [2004], Logothetis et al. [2001]).

However, other evidence suggests that a radial bias may be neurally fundamental. First, psychophysical data strongly confirms a radial bias in perception (Figures 1 and 4; Bennett and Banks, 1991; Berardi and Fiorentini, 1991; Fahle, 1986; McGraw and Whitaker, 1999; Rovamo et al., 1982; Scobey and van Kan, 1991; Temme et al., 1985; Westheimer, 2003, 2005; Yap et al., 1987), so it is less surprising to see this reflected in the fMRI. Second, the fMRI evidence for a radial bias was obvious in both macaques and humans, and it survived an extensive series of control tests in humans. Finally, the fact that the present fMRI evidence was found in all retinotopic areas also suggests that it reflects a basic feature of overall visual perception. Consider the alternative: imagine that the present result reflects a peculiar discrepancy between a presynaptic radial bias (reflected by the fMRI) which is then somehow nulled at the immediately higher processing level (e.g., extracellular action potentials, measured by single unit recording in the postsynaptic neurons). Such a specific hypothetical discrepancy could be maintained only in a single visual cortical area, not in downstream areas—and this is ruled out by the ubiquity of the present fMRI bias throughout visual cortex.

It is also possible that previous investigators were simply not looking for, nor expecting to find, a radial orientation bias. For instance, many single-unit studies have carefully measured and plotted orientation tuning curves, reporting little or no orientation bias. However, most electrophysiological studies measured *absolute* orientation in different parts of the visual field, not *polar* orientation (i.e., orientation relative to the center of gaze). The present results would only be revealed by polar analysis. In fact, electrophysiological studies which did test polar orientation also reported a radial orientation bias (Durand et al., 2002, 2004; Leventhal, 1983). Recent reports of a subtle orientation selectivity in human fMRI data (e.g., Kamitani and Tong [2005]) also assumed

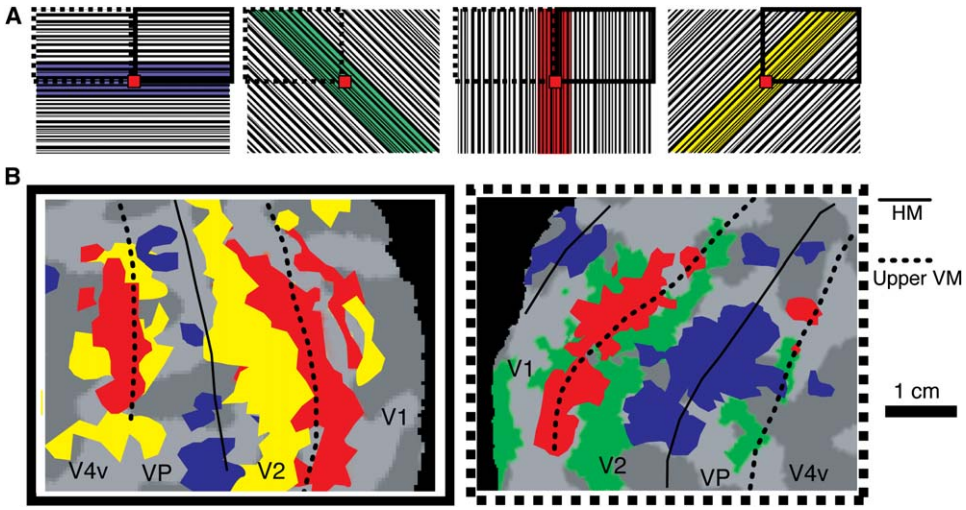

Figure 7. fMRI Activity Produced by Oblique Orientations Is Significantly Higher along the Representation of Corresponding Retinotopic Polar Angles

(A) Examples of the orientations tested. Superimposed on the actual stimuli are the regions of the visual field represented in cortex (B) (dashed line = left upper visual field, right inferior visual cortex; solid line = right upper visual field, left inferior visual cortex). Red, green, yellow, and blue pseudocolor highlight the location of the radial stimulus stripes in each stimulus.

(B) Magnified view of maximal fMRI activity in the flattened inferior left and right hemispheres (on the left and right, respectively), produced by gratings of either vertical (red), horizontal (blue), or oblique (green = left-leaning, or yellow = right-leaning) orientation. Corresponding representations of the retinotopic meridians are indicated in the same subject's cortex as solid and dotted lines. The activity produced by each grating was subtracted against that produced by the otherwise-equivalent grating at the orthogonal orientation.

no orientation bias, but the present orientation bias also predicts those results. Even the data from optical imaging studies does not rule out the present radial bias, because such data is often filtered in such a way that any global orientation biases are removed (e.g., Shmuel and Grinvald [1996]).

So how does the radial orientation bias fit into existing neural models? Leventhal et al. (Leventhal, 1983; Shou and Leventhal, 1989) pointed out that a radial bias might arise naturally, since retinal ganglion cells (and dendritic arborization) are added radially as the eye grows during development (Leventhal and Schall, 1983; Rodieck et al., 1985; Schall and Leventhal, 1987; Schall et al., 1986). A radial bias could also arise from other developmental factors, since radial orientations are the only orientations not blurred by saccades to a given retinotopic location (disregarding saccadic suppression). Westheimer (2003) suggested that a radial cortical bias might underlie perceptual distortions during eye torsion. Durand et al. (2004) emphasized the usefulness of radial

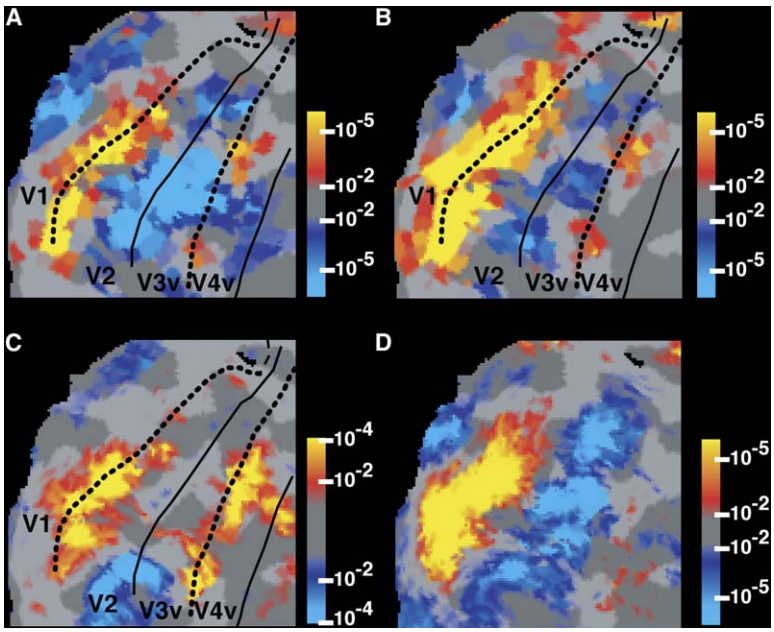

Figure 8. Control Tests Clarify the Radial Orientation Bias in Human Visual Cortex

These four panels show fMRI maps taken from the same subject, in the flattened inferior right hemisphere. In all panels, the stimuli and activity format are as described in Figure 6.

(A) Relative activity during passive viewing conditions.

(B) Analogous activity while subjects concurrently performed an attention control experiment.

(C) Activity when gratings were presented in event-related format (stimulus duration = 1 s; ISI = 1–22 s).

(D) Activity when averaged across all subjects, with cortical surfaces aligned according to anatomical (gyral/sulcal) landmarks (e.g., Dale et al. [1999], Fischl et al. [1999]); thus, individual retinotopic borders are not shown. Although there is some variability in results across the different scan sessions, the basic result is similar in all conditions: vertical orientations produce highest activity (red-yellow) along the vertical retinotopic meridian (dotted lines), and horizontal orientations produce highest activity (blue-cyan) along the horizontal meridian (solid lines).

orientations in computations of binocular disparity. The "local-global map hypothesis" (Alexander et al., 2004) also proposed a global radial bias for orientation, to facilitate contextual integration in V1. The radial bias also has obvious relevance for calculation of optic flow and saccades.

Obviously, more work will be required to understand this orientation bias. However, the present evidence demonstrates clearly that there are specific links between orientation tuning and the underlying cortical retinotopy, which have not been previously appreciated.

Experimental Procedures

Psychophysics

Four subjects, with normal or corrected-to-normal vision, participated in this experiment. The subjects were placed in a dimly lit room (with the monitor as the only light source) and viewed the displays binocularly. Subjects were required to fixate the center of the monitor screen at all times. The distance between the eyes and screen was 57 cm. Images were displayed on a monitor with linear display characteristics (1024 × 768 pixels, 60 Hz refresh rate). The luminance of the gray background was 6.74 cd/m^2.

Stimuli were low-contrast sinusoidal gratings presented inside a small square aperture (1.2° × 1.2°). The spatial frequency was fixed at 4 cycles/degree. In each experimental block, the grating patches were presented in a single visual field location, centered at 15.5° from the fixation point. Relative to the fixation point, the polar angle of the stimulus location was either 0° (right-horizontal), 45° (upper-right), 90° (upper vertical), 135° (upper-left), 180° (left-horizontal), 225° (lower-left), 270° (lower-vertical) or 315° (lower-right). Thus, the grating of 45° orientation corresponded to a radial orientation in the upper left visual position, and a tangential orientation in the upper right visual position. Each block contained 60 trials. Each trial consisted of three successive 250 ms intervals, indicated by changes in the color of the fixation point. The grating stimulus was presented randomly during either the first interval (fixation point, green) or the third interval (fixation point, yellow). The second interval was blank. The orientation of the sine grating was either radial or tangential relative to the fixation point, selected randomly in each trial. Subjects had to indicate (during the 2000 ms intertrial interval; fixation point, red) whether it was the first or the third interval that had contained the grating (temporal two-alternative forced-choice paradigm).

Contrast threshold was measured using a staircase method. The initial stimulus contrast was 10%. The contrast was decreased after every three successive correct responses, and increased after every single incorrect response. The step for each change in the contrast was equal to 1%. Using this rule, the stimulus level approached the point at which the observers were 79% correct. The average of the last five trials was taken as the threshold. Two independent staircases were run in each block (for each radial and tangential orientation). Subjects completed at least two blocks for each visual field quadrant. At the beginning of the experimental session, each subject practiced for one block.

Visual Stimuli for fMRI

Stimuli were generated on a PC and presented via LCD projector (Sharp NoteVision 6, resolution = 1024 × 768). A small central fixation point was superimposed on all grating stimuli. Gratings were of high (>95%) contrast, rectangular in cross-sectional waveform. In most of the gratings (e.g., Figures 3 and 5–7), stripe width (for both black and white stripes) was varied randomly between 0.13° and 0.64° across the display (32.9° × 24.7°). A subset of gratings (e.g., Figure S1) were radial or concentric instead of rectilinear; some of those stripe patterns were scaled with eccentricity (log-polar). In these concentric/radial stimuli, the stripe width varied linearly with eccentricity. Except as noted, a given grating was presented for 0.5 s, then the contrast-reversed grating was presented for the following 0.5 s, and the grating was recalculated at a new (random) phase for the next presentation. In the block design experiments, the local orientation was kept constant throughout each block (typically 16 s duration).

Retinotopic mapping stimuli were contrast-counterphased, scaled checkerboard stimuli confined to polar ring- or ray-shaped apertures, as described previously in humans (Engel et al., 1994; Sereno et al., 1995; Tootell et al., 1997) and monkeys (Fize et al., 2003).

Imaging Procedure, Human Subjects

Human subjects were scanned in a 3T MRI (Siemens, Allegra), using a single-shot, gradient echo EPI sequence optimized for BOLD contrast. For this study, 762,800 functional images (30,512 functional volumes, typically 1728 volumes/subject/session) were obtained from six subjects (25 slices oriented perpendicular to the calcarine fissure, voxel size = 3 mm^3 isotropic, TE = 30 ms, flip angle 90°). The TR was 2 s for all scans except the retinotopic scans (TR = 4 s). The functional scans were done using a custom-built, semicylindrical surface coil, which yielded high sensitivity over all of occipital and posterior parietal and temporal cortex. All six fMRI subjects gave written consent and the experimental protocol was approved by MGH-IRB. All subjects had normal or corrected-to-normal vision, and showed high-quality fMRI maps of retinotopy as a prerequisite for the subsequent tests of orientation sensitivity.

High-resolution 3D anatomical MR images (MP-RAGE) were also acquired, for use in subsequent reconstruction of cortex in flattened format (Dale et al., 1999; Fischl et al., 1999). Such scans (TR = 2.531 s, TE = 3.28 ms, flip angle = 7°, TI = 1100 ms, 256 slices, voxel size = 1.3 × 1.3 × 1 mm, resliced during analysis to 1 mm^3 isotropic) were acquired using a head coil with near-uniform coverage of the entire brain.

In an additional scan session, functional MR images were taken to define the borders of different visual areas. A phase encoded retinotopic mapping approach (Sereno et al., 1995) was used to define retinotopic areas V1, V2, V3, VP, V4v, V3A. Area MT+ was defined using low-contrast moving stimuli (Tootell et al., 1995). Area V4d was defined by cortical topography, based on the position of neighboring areas V3, V3A, V4v, and MT+ (Tootell and Hadjikhani, 2001). LO and V8 were not consistently localized in this study, so data from those regions were not analyzed here.

Remaining sessions were devoted to the main studies of orientation sensitivity. Except in event-related controls (e.g., Figure 8), we used block-design paradigms because of their high sensitivity. Typically, three conditions (two main conditions and one control) were compared in each scan (18 blocks, 16 seconds/block, order randomized). The main grating conditions included (1) vertical versus horizontal (e.g., Figure 6); (2) oblique orientation versus orthogonal oblique orientation (e.g., Figures 2, 3, and 8); (3) radial versus concentric or concentric versus rectilinear (e.g., Figure S1). Some experiments included control blocks of spatially uniform gray, as a measure of baseline activity.

Throughout all scans (including attention-related controls), subjects were instructed to maintain gaze on the central fixation point.

Attention Control

To control for variations in attention, additional experiments were conducted in which subjects (n = 5) performed a detection task during presentation of the grating stimuli. The same subjects used in the passive viewing experiments participated in the attention controls, except for a single subject who was no longer available.

In this condition, each subject was cued (by the stimulus contrast change, once per second) to respond (via a button box located inside the scanner) by pressing button 1 if a small (0.2° × 0.2°) red probe dot was present in the display and button 2 if it was absent. The probe dot was present in 50% of the trials, randomly ordered. When present, the probe dot appeared and disappeared coincident with a grating refresh and/or contrast reversal. When present, the probe dot could appear anywhere in the display (with equal spatial weighting), except that the dot appeared only on the white stripes, not the black. To achieve optimal performance, subjects had to attend carefully to the full retinotopic extent of the grating.

The detectability of the probe dot was manipulated by varying its red/white ratio (decreased saturation = decreased detection). Threshold was modulated by the staircase method (converging on 68% correct), to keep subjects' performance level constant, and to prevent pop-out effects. Except for the probe dot, the stimulus was equivalent to the other grating stimuli. The subjects' performance

was equated across different grating conditions. The length of each grating presentation was 1 s for each contrast.

Event-Related Control

Gratings of either vertical or horizontal orientation were presented in randomized order, with an intervening baseline condition of spatially uniform gray. Gratings were presented as a contrast-reversed pair (0.5 s each contrast, total grating duration 1 s) separated from the next grating by a variable ISI (1–22 s).

Data Analysis

Data were analyzed by FS-FAST and FreeSurfer (http://surfer.nmr.mgh.harvard.edu). All the functional images were motion corrected (Cox and Jesmanowicz, 1999), spatially smoothed with a Gaussian kernel of 2.5 mm (HWHM), and normalized across sessions individually. The average signal intensity maps were then calculated for each condition, for each individual subject. The voxel-by-voxel statistical tests were conducted by computing contrasts based on a univariate general linear model. The significance levels were projected onto the flattened cortex individually and computed using a fixed-effects model. For the averaging across subjects, each individual subjects' functional data were spatially normalized using the spherical transformation (Dale et al., 1999; Fischl et al., 1999). This procedure aligns cortical surfaces from different subjects according to MRI-based anatomical sulci and gyri, but not functional (e.g., retinotopic area) boundaries.

Imaging Procedure, Macaque Monkeys

Two male rhesus monkeys (3–4.5 kg) were scanned, in the same MRI scanner used in the human experiments (3 T Siemens Allegra). The whole brain was included in these scans, using a single loop coil of 11 cm diameter. The monkey data included 410,550 functional images (20,770 functional volumes, 240 volumes/scan, typically 2880 volumes/session). To reduce susceptibility artifacts due to gross body motion, we used a multiecho sequence (Greve et al., 2003), with a flip angle of 90° and a TE of 32 and 73 ms. For the tests of orientation sensitivity, we used 18 slices, TR = 2 s, and a voxel size of 1.5 mm^3 isotropic. The control maps of retinotopy included a larger cortical area (22–31 slices, TR = 3–4 s, voxel size = 1.25–1.5 mm^3 isotropic).

As described elsewhere (Leite et al., 2002; Tsao et al., 2003a, 2003b; Vanduffel et al., 2002), all monkeys were scanned while awake and fixating the center of the stimuli, using operant conditioning with liquid (water/apple juice) rewards. Sensitivity was increased by using an exogenous contrast agent (MION, 7 mg/kg IV). An eye movement monitor (modified ISCAN) furnished on-line, artifact-free records of fixation stability within the scanner. During scanning, the monkeys were physically constrained in the "sphinx" position within a restraint device (Primatrix Co.), inside the MR bore. Additional procedures are as described elsewhere (Leite et al., 2002; Tsao et al., 2003a, 2003b). All procedures were approved by Massachusetts General Hospital SRAC protocol, in accordance with NIH guidelines.

Data analysis for the macaque fMRI was equivalent to that used in the human fMRI, with the following exceptions. The smoothing step was eliminated, consistent with the smaller size of the monkey brain and the increased spatial resolution of the monkey fMRI procedures. The time course and polarity of the MRI response was based on an estimate of the MION response, rather than the BOLD response.

Supplemental Data

The Supplemental Data for this article can be found online at http://www.neuron.org/cgi/content/full/51/5/661/DC1/.

Acknowledgments

This work was supported by NIH grants MH67529, EB00790, P41RR14075, the MIND Institute, and the Athinoula A. Martinos Center for Biomedical Imaging. We thank Gerald Westheimer, Guy Orban, Doris Tsao, Jeffrey Schall, and Yukiyasu Kamitani for helpful discussions. We also thank Tamara Knutsen for help with the monkey fMRI and Anders Dale and Anna Devor for their assistance with the distortion correction procedure in the monkey fMRI data.

Received: February 23, 2006
Revised: May 31, 2006
Accepted: July 25, 2006
Published: September 6, 2006

References

Albrecht, D.G., De Valois, R.L., and Thorell, L.G. (1980). Visual cortical neurons: are bars or gratings the optimal stimuli? Science *207*, 88–90.

Alexander, D.M., Bourke, P.D., Sheridan, P., Konstandatos, O., and Wright, J.J. (2004). Intrinsic connections in tree shrew V1 imply a global to local mapping. Vision Res. *44*, 857–876.

Bennett, P.J., and Banks, M.S. (1991). The effects of contrast, spatial scale, and orientation on foveal and peripheral phase discrimination. Vision Res. *31*, 1759–1786.

Berardi, N., and Fiorentini, A. (1991). Visual field asymmetries in pattern discrimination: a sign of asymmetry in cortical visual field representation? Vision Res. *31*, 1831–1836.

Berkley, M.A., Kitterle, F., and Watkins, D.W. (1975). Grating visibility as a function of orientation and retinal eccentricity. Vision Res. *15*, 239–244.

Cox, R.W., and Jesmanowicz, A. (1999). Real-time 3D image registration for functional MRI. Magn. Reson. Med. *42*, 1014–1018.

Dale, A.M., Fischl, B., and Sereno, M.I. (1999). Cortical surface-based analysis. I. Segmentation and surface reconstruction. Neuroimage *9*, 179–194.

De Valois, R.L., Albrecht, D.G., and Thorell, L.G. (1982a). Spatial frequency selectivity of cells in macaque visual cortex. Vision Res. *22*, 545–559.

De Valois, R.L., Yund, E.W., and Hepler, N. (1982b). The orientation and direction selectivity of cells in macaque visual cortex. Vision Res. *22*, 531–544.

Durand, J.B., Zhu, S., Celebrini, S., and Trotter, Y. (2002). Neurons in parafoveal areas V1 and V2 encode vertical and horizontal disparities. J. Neurophysiol. *88*, 2874–2879.

Durand, J.B., Celebrini, S., and Trotter, Y. (2004). Neural correlates of the induced effect, based on vertical disparity and orientation selectivities in area V1. Paper presented at 34th annual meeting, Society for Neuroscience, San Diego, California.

Engel, S.A., Rumelhart, D.E., Wandell, B.A., Lee, A.T., Glover, G.H., Chichilnisky, E.J., and Shadlen, M.N. (1994). fMRI of human visual cortex. Nature *369*, 525.

Fahle, M. (1986). Curvature detection in the visual field and a possible physiological correlate. Exp. Brain Res. *63*, 113–124.

Fischl, B., Sereno, M.I., and Dale, A.M. (1999). Cortical surface-based analysis. II: Inflation, flattening, and a surface-based coordinate system. Neuroimage *9*, 195–207.

Fize, D., Vanduffel, W., Nelissen, K., Denys, K., Chef d'Hotel, C., Faugeras, O., and Orban, G.A. (2003). The retinotopic organization of primate dorsal V4 and surrounding areas: a functional magnetic resonance imaging study in awake monkeys. J. Neurosci. *23*, 7395–7406.

Frisen, L., and Glansholm, A. (1975). Optical and neural resolution in peripheral vision. Invest. Ophthalmol. *14*, 528–536.

Furmanski, C.S., and Engel, S.A. (2000). An oblique effect in human primary visual cortex. Nat. Neurosci. *3*, 535–536.

Greve, D.N., van der Kouwe, A., West, C., and Dale, A.M. (2003). Weighting of multiple gradient echo images to improve detection of fMRI activation. Paper presented at Human Brain Mapping, New York, New York.

Haynes, J.D., and Rees, G. (2005). Predicting the orientation of invisible stimuli from activity in human primary visual cortex. Nat. Neurosci. *8*, 686–691.

Hubel, D.H., and Wiesel, T.N. (1962). Receptive fields, binocular interaction and functional architecture in the cat's visual cortex. J. Physiol. *160*, 106–154.

Kamitani, Y., and Tong, F. (2005). Decoding the visual and subjective contents of the human brain. Nat. Neurosci. *8*, 679–685.

Kim, D.S., Ronen, I., Olman, C., Kim, S.G., Ugurbil, K., and Toth, L.J. (2004). Spatial relationship between neuronal activity and BOLD functional MRI. Neuroimage *21*, 876–885.

Leite, F.P., Tsao, D., Vanduffel, W., Fize, D., Sasaki, Y., Wald, L.L., Dale, A.M., Kwong, K.K., Orban, G.A., Rosen, B.R., et al. (2002). Repeated fMRI using iron oxide contrast agent in awake, behaving macaques at 3 Tesla. Neuroimage *16*, 283–294.

Leventhal, A.G. (1983). Relationship between preferred orientation and receptive field position of neurons in cat striate cortex. J. Comp. Neurol. *220*, 476–483.

Leventhal, A.G., and Schall, J.D. (1983). Structural basis of orientation sensitivity of cat retinal ganglion cells. J. Comp. Neurol. *220*, 465–475.

Levick, W.R., and Thibos, L.N. (1982). Analysis of orientation bias in cat retina. J. Physiol. *329*, 243–261.

Logothetis, N.K., Pauls, J., Augath, M., Trinath, T., and Oeltermann, A. (2001). Neurophysiological investigation of the basis of the fMRI signal. Nature *412*, 150–157.

Mansfield, R.J. (1974). Neural basis of orientation perception in primate vision. Science *186*, 1133–1135.

McGraw, P.V., and Whitaker, D. (1999). Perceptual distortions in the neural representation of visual space. Exp. Brain Res. *125*, 122–128.

Movshon, J.A., Thompson, I.D., and Tolhurst, D.J. (1978). Spatial summation in the receptive fields of simple cells in the cat's striate cortex. J. Physiol. *283*, 53–77.

Orban, G.A., Vandenbussche, E., and Vogels, R. (1984). Human orientation discrimination tested with long stimuli. Vision Res. *24*, 121–128.

Ringach, D.L., Hawken, M.J., and Shapley, R. (1997). Dynamics of orientation tuning in macaque primary visual cortex. Nature *387*, 281–284.

Rodieck, R.W., Binmoeller, K.F., and Dineen, J. (1985). Parasol and midget ganglion cells of the human retina. J. Comp. Neurol. *233*, 115–132.

Rovamo, J., Virsu, V., Laurinen, P., and Hyvarinen, L. (1982). Resolution of gratings oriented along and across meridians in peripheral vision. Invest. Ophthalmol. Vis. Sci. *23*, 666–670.

Sasaki, Y., Hadjikhani, N., Fischl, B., Liu, A.K., Marrett, S., Dale, A.M., Tootell, R.B., and Marret, S. (2001). Local and global attention are mapped retinotopically in human occipital cortex. Proc. Natl. Acad. Sci. USA *98*, 2077–2082.

Schall, J.D., and Leventhal, A.G. (1987). Relationships between ganglion cell dendritic structure and retinal topography in the cat. J. Comp. Neurol. *257*, 149–159.

Schall, J.D., Perry, V.H., and Leventhal, A.G. (1986). Retinal ganglion cell dendritic fields in old-world monkeys are oriented radially. Brain Res. *368*, 18–23.

Schoups, A., Vogels, R., Qian, N., and Orban, G. (2001). Practising orientation identification improves orientation coding in V1 neurons. Nature *412*, 549–553.

Scobey, R.P., and van Kan, P.L. (1991). A horizontal stripe of displacement sensitivity in the human visual field. Vision Res. *31*, 99–109.

Sereno, M.I., Dale, A.M., Reppas, J.B., Kwong, K.K., Belliveau, J.W., Brady, T.J., Rosen, B.R., and Tootell, R.B. (1995). Borders of multiple visual areas in humans revealed by functional magnetic resonance imaging. Science *268*, 889–893.

Shmuel, A., and Grinvald, A. (1996). Functional organization for direction of motion and its relationship to orientation maps in cat area 18. J. Neurosci. *16*, 6945–6964.

Shou, T.D., and Leventhal, A.G. (1989). Organized arrangement of orientation-sensitive relay cells in the cat's dorsal lateral geniculate nucleus. J. Neurosci. *9*, 4287–4302.

Temme, L.A., Malcus, L., and Noell, W.K. (1985). Peripheral visual field is radially organized. Am. J. Optom. Physiol. Opt. *62*, 545–554.

Tootell, R.B., and Hadjikhani, N. (2001). Where is 'dorsal v4' in human visual cortex? retinotopic, topographic and functional evidence. Cereb. Cortex *11*, 298–311.

Tootell, R.B., Silverman, M.S., Hamilton, S.L., Switkes, E., and De Valois, R.L. (1988). Functional anatomy of macaque striate cortex. V. Spatial frequency. J. Neurosci. *8*, 1610–1624.

Tootell, R.B., Reppas, J.B., Dale, A.M., Look, R.B., Sereno, M.I., Malach, R., Brady, T.J., and Rosen, B.R. (1995). Visual motion aftereffect in human cortical area MT revealed by functional magnetic resonance imaging. Nature *375*, 139–141.

Tootell, R.B., Mendola, J.D., Hadjikhani, N.K., Ledden, P.J., Liu, A.K., Reppas, J.B., Sereno, M.I., and Dale, A.M. (1997). Functional analysis of V3A and related areas in human visual cortex. J. Neurosci. *17*, 7060–7078.

Tsao, D.Y., Freiwald, W.A., Knutsen, T.A., Mandeville, J.B., and Tootell, R.B. (2003a). Faces and objects in macaque cerebral cortex. Nat. Neurosci. *6*, 989–995.

Tsao, D.Y., Vanduffel, W., Sasaki, Y., Fize, D., Knutsen, T.A., Mandeville, J.B., Wald, L.L., Dale, A.M., Rosen, B.R., Van Essen, D.C., et al. (2003b). Stereopsis acitivates V3A and caudal intraparietal areas in macaques and humans. Neuron *39*, 555–568.

Vanduffel, W., Fize, D., Mandeville, J.B., Nelissen, K., Van Hecke, P., Rosen, B.R., Tootell, R.B., and Orban, G.A. (2001). Visual motion processing investigated using contrast agent-enhanced fMRI in awake behaving monkeys. Neuron *32*, 565–577.

Vanduffel, W., Tootell, R.B., Schoups, A.A., and Orban, G.A. (2002). The organization of orientation selectivity throughout macaque visual cortex. Cereb. Cortex *12*, 647–662.

Westheimer, G. (2003). The distribution of preferred orientations in the peripheral visual field. Vision Res. *43*, 53–57.

Westheimer, G. (2005). Anisotropies in peripheral vernier acuity. Spat. Vis. *18*, 159–167.

Yap, Y.L., Levi, D.M., and Klein, S.A. (1987). Peripheral hyperacuity: isoeccentric bisection is better than radial bisection. J. Opt. Soc. Am. A *4*, 1562–1567.